Journal of Radioanalytical and Nuclear Chemistry (2021) 329:555–564
https://doi.org/10.1007/s10967-021-07723-x

Preparation of phosphate-functionalized biopolymer/graphene oxide gels for enhanced selective adsorption of U(VI) from aqueous solution

Lijiao Fan[1] · Guolin Huang[1] · Shasha Yang[1] · Yiming Xie[1] · Wenbing Liu[1] · Jeffery Shi[2]

Received: 3 January 2021 / Accepted: 9 April 2021 / Published online: 7 June 2021

Abstract

The adsorption properties of phosphate-functionalized biopolymer/graphene oxide gels on U(VI) in aqueous solution were studied. The characterization of prepared gels were measured by scanning electron microscopy (SEM), Energy dispersive spectroscopy (EDS), Fourier transformed infrared spectra (FT–IR), and X-ray diffraction (XRD). The adsorption of U(VI) was evaluated as a function of the pH of solution, initial uranium concentration and the contact time, and the optimum conditions for U(VI) adsorption was obtained. The Langmuir isotherm model fits the experimental data very well, and the maximum uptake of U(VI) were 568.18 mg/g for P-TA-GO and 546.45 mg/g for P-AL-GO, respectively. The experimental data for the kinetics of adsorption correlated well with the second-order Langergren rate equation, and Langergren rate constants have been determined. Compared to other coexisting ions present in real-world uranium-containing wastewater, the phosphate-functionalized biopolymer/graphene oxide gels have demonstrated remarkably better selective adsorption to U(VI).

Keyword Phosphate-functionalized · Graphene oxide · Uranium · Adsorption · Kinetic

List of symbols

C_o	U(VI) ion concentration in the initial solution (mg L^{-1})
c_e	U(VI) ion concentration at equilibrium (mg L^{-1})
ΔG^0	Change in the Gibbs free energy (J mol^{-1})
ΔH^0	Change in standard enthalpy (J mol^{-1})
K_1	Rate constant (L min^{-1})
K_2	Rate constant (g mg^{-1} min^{-1})
K_d	Distribution constant (mL g^{-1})
$K_{d,M}$	Distribution coefficient of U(VI) and the competing metal ion (L g^{-1})
$K_{d,U}$	Distribution coefficient of U(VI) and the competing metal ion (L g^{-1})
K_F	Constant of Freundlich model (mg g^{-1})
K_L	Constant of Langmuir model (L mg^{-1})
m	Weight of adsorbent (g)
n	Freundlich linearity index
q_e	Amount of U(VI) ion adsorbed at equilibrium (mg g^{-1})
q_m	Theoretical maximum adsorption capacity per unit weight of the adsorbent (mg g^{-1})
q_t	Amount of U(VI) ion adsorbed at time t (mg g^{-1})
R	Universal gas constant (8.314 J mol^{-1} K^{-1})
ΔS^0	Change in standard entropy(J mol^{-1} K^{-1})
$S_{U/M}$	Distribution selectivity coefficient
T	Temperature (K)
t	Time (s)
v	Volume of the solution (L

✉ Guolin Huang
guolinhuang@sina.com

[1] State Key Laboratory of Nuclear Resources and Environment, East China University of Technology, Nanchang 330013, China

[2] School of Chemical and Biomolecular Engineering, The University of Sydney, Sydney 2006, Australia

Introduction

Uranium-containing wastewater represents a seriously threat to ecological system and human health. The research conducted in this area points to the urgent need of technologies that are effective for uranium removal or to prevent the release of uranium into the environment [1]. Currently, many remediation technologies for the treatment of uranium, including ion exchange processes [2], chemical coagulation-flocculation [3], extraction [4, 5], biosorption [6], hydrogel membrane processes [7], and adsorption [8, 9], have been proposed, assessed and studied. Among them, adsorption techniques have especially attracted outstanding attentions

because of their advantages on feasibility, efficiency and simple operation.

Graphene oxide (GO), has been considered as one of the most efficient adsorbents for uranium removal [10]. The coacervation caused by the use of GO slows down the adsorption process and reduces the adsorption capacity. GO-biopolymer gels with interconnected porous structures prepared by biopolymers as polymeric crossing agents [11, 12]. As described in our previous work, chitosan (CS), sodium carboxymethyl cellulose (CMC) and bovine serum albumin (BSA) grafted on to the surface of GO provide effective adsorption of uranium [13, 14]. Sodium alginate (AL) and Tannin (TA) have been reported that could produce a strong ability of combination for metal ions due to its existence of extremely abundant and multiple adjacent phenolic hydroxyl groups [15].

Different ions including Nd^{3+}, La^{3+}, Ce^{3+}, Sr^{2+}, Ni^{2+}, Co^{2+} and Ba^{2+} often coexists in uranium-containing wastewater, so it is needed to enhance the selective adsorption for uranium over coexisting ions. Amidoxime was used with GO-biopolymer gels to improve the selectivity of uranium adsorption as the function of its effective chelating groups as reported in our previous work [16]. It has been found that phosphoryl groups have the high affinity to uranium [17]. Therefore, the phosphate-functionalized biopolymer/graphene oxide gels may be regarded as excellent adsorbents with high selective adsorption of uranium.

Preparation of phosphate-functionalized biopolymer (Sodium alginate, Tannin)/GO gels and their application in selective adsorption of U(VI) from aqueous solution are the focus of this study. The adsorption behaviors of uranium on P-AL-GO/P-TA-GO were systematically evaluated under various process conditions including solution pH, initial concentrations and contact time to obtain the most suitable conditions. Mechanism of uranium removal was also investigated through the development of adsorption kinetic models, measuring adsorption isotherms, and the determination of adsorption thermodynamic parameters based on the data obtained by the batch adsorption experiments.

Materials and methods

Preparation of sodium alginate-graphene oxide (AL-GO)

50 mg of GO was ultrasonically dispersed in 100 mL of deionized water, the solution was sonicated for 10 min. 1.0 g of sodium alginate was added to the GO solution, and magnetically stirred until uniformly mixed to obtain an AL-GO solution. The solution was then added to 200 mL $CaCl_2$ solution with a concentration of 10 mg/mL by using a syringe. The resulting solution was placed at 4 °C overnight. The suspension were washed with deionized water until being neutralized, followed by being rinsed with pure alcohol for 3 times. The obtained product was dried in a vacuum oven at 60 °C for overnight.

Preparation of tannin-graphene oxide (TA-GO)

100 mg of GO was ultrasonically dispersed in 100 mL of deionized water, the solution was sonicated for 10 min. 2.0 mL of glutaraldehyde was added to the GO solution, and magnetically stirred for 4 h until uniformly mixed. 100 mg of tannin was dispersed in 50 mL of deionized water, and then was added to the GO solution. The resulting solution was heated to the temperature of 50 °C and stirred for 4 h. The product was washed and dried.

Preparation of phosphate-functionalized AL-GO/TA-GO

0.5 g of AL-GO/TA-GO and 35 mL of concentrated phosphoric acid were dispersed in a 100 mL beaker, and had been reacted at 50 °C for 12 h. The suspension were washed alternately with deionized water and pure alcohol. After drying, thus obtained products were referred as P-AL-GO/P-TA-GO gels in the paper.

A stock solution of U(VI) solution with concentration of 1 mg mL^{-1} by dissolving 1.1792 (±0.0001) g of U_3O_8 (dried at 105 °C for 2 h) by deionized water in a 1000 mL flask. 10 mg of the adsorbents were transferred into a 20 mL of U(VI) solution with known concentration and pH value in a flask. The pH of the suspension was adjusted to be in the range of 2.0–6.5 by adding negligible volumes of 0.1 mol/L H_2SO_4 and 0.1 mol/L NaOH solution. After filtration, these adsorbents were collected from the solution with a permanent magnet. The concentration of U(VI) in the solution was determined by the UV- visible spectrophotometer using arsenazo III method. The adsorption capacity of U(VI) was calculated by the following Eq. (1):

$$q_m = \frac{(C_0 - C_e)v}{m} \quad (1)$$

The Infrared spectra were used to study the function groups (Nicolet IS10, Thermo Scientific Brand, USA). The SEM images were taken using a Nova Nano scanning electron microscopy 450 (FEI Co., Ltd., USA). XRD patterns were measured on D8-A25 (Bruker Instrument Co., Ltd., Germany). The EDS analysis was conducted on EX-250x (Horiba Co., Ltd., Japan). The surface zeta potential of the composite was measured using a potential analyzer (Stabino PMX 400, Micotrac, USA).

Result and discussion

The SEM images of AL-GO/ Ta-GO, P-AL-GO/P-TA-GO were depicted in Fig. 1. Figure 1a (for AL-GO) and Fig. 1b (for TA-GO) show that the surface of GO with cross-linked structure as sodium alginate and tannin have certain mechanical strength and fixed shape, which indicated a good modification effect. Compared with AL-GO/TA-GO, the microstructure of phosphorylated P-AL-GO/ P-TA-GO changed from the shape of beads to a large number of stacked fragments, and the surface roughness increased, which is good for subsequent adsorption of U(VI), as depicted in Fig. 1c and d. After phosphorylation, the surface of the adsorbent displayed significant changes, demonstrating the effectiveness of the modification process.

Figure 2 shows the FTIR spectra of GO, Al-GO/TA-GO, and P-AL-GO/P-TA-GO. As shown, the presence of pure GO results in the display of its characteristic peaks at 3200 cm^{-1} (O–H), 1730 cm^{-1} (O=H), 1404 cm^{-1} (C–OH), 1235 cm^{-1} (C–O–C), and 1044 cm^{-1} (C–O). For the AL-GO, the characteristic peaks at 1584 cm^{-1} and 1408 cm^{-1} are results of asymmetric and symmetric tensile vibrations of $–COO^{-}$. The most logical explanation for these two peaks is the cross-linking between GO and sodium alginate. The presence of characteristic peaks at 3356 cm^{-1} (O–H), 1730 cm^{-1} (O=H), 1360 cm^{-1} (C–O–C), and 1020 cm^{-1} (C–O) indicate the cross-linking of GO and TA in the TA-GO. The new peaks at 1211 cm^{-1}/1020 cm^{-1} (for P-AL-GO) and 961 cm^{-1} (for P-TA-GO) corresponds to the vibration of P-O, which suggests the occurrence of phosphate-functionalization process in the preparation of P-AL-GO/ P-TA-GO gels.

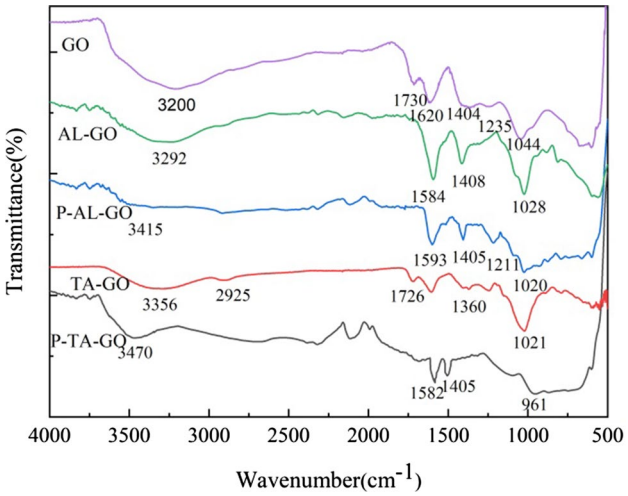

Fig. 2 FT-IR spectra of GO, Al-GO/TA-GO, and P-AL-GO/P-TA-GO

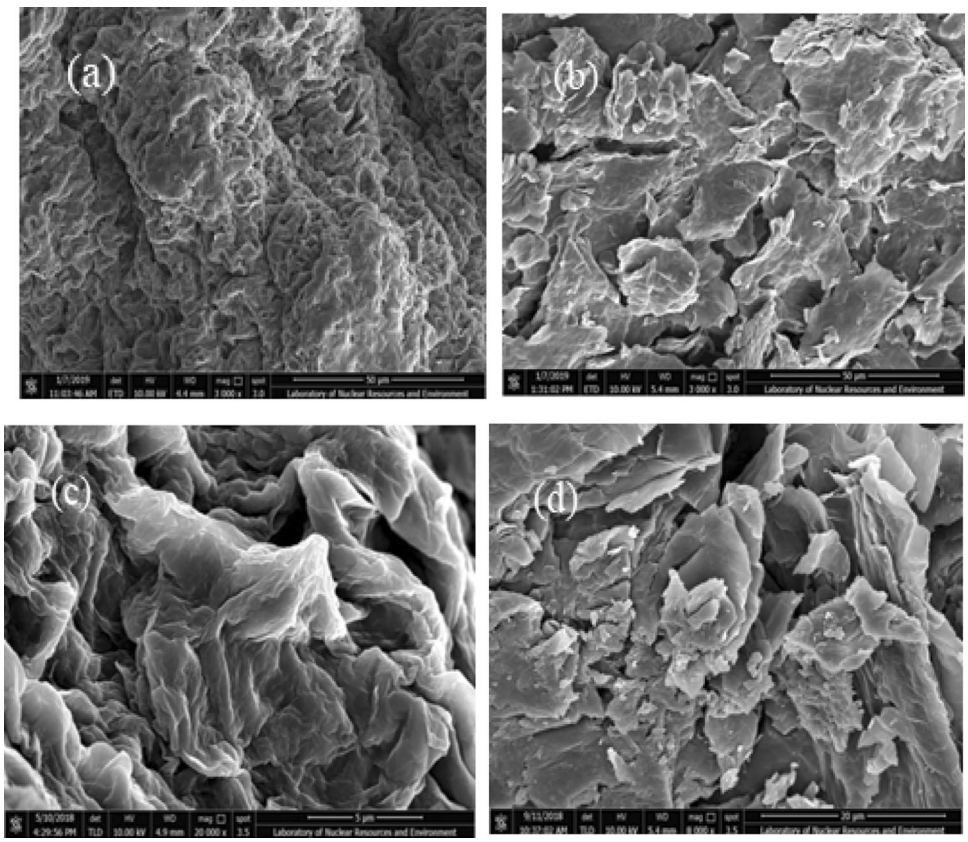

Fig. 1 SEM images of AL-GO (**a**) /TA-GO(**b**), P-AL-GO(**c**) / P-TA-GO(**d**)

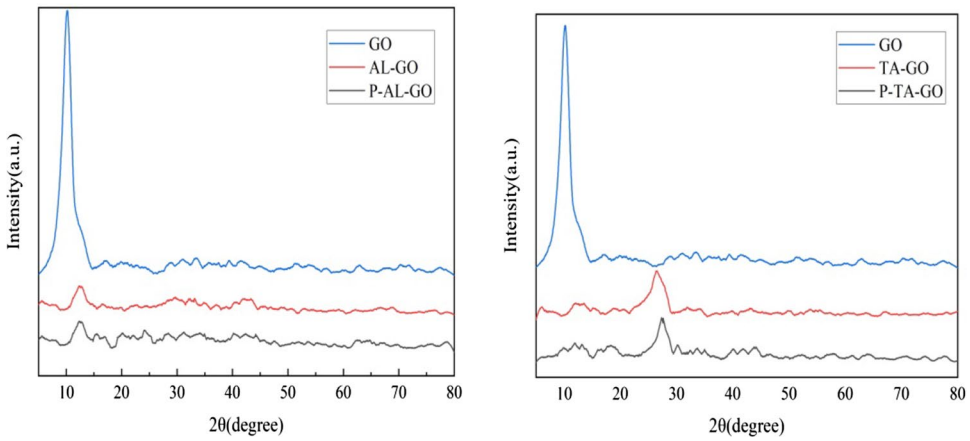

Fig. 3 XRD pattern of AL-GO/P-AL-GO (right) and TA-GO/P-TA-GO (left)

XRD measurements were employed to check whether the preparation process were successful. The XRD are shown in Fig. 3. The peak at 10.3° in GO can be attributed the characteristic diffraction peak of crystalline structure of GO. A moderately strong peak at 12.2° in AL-GO and a sharp peak appear at 26.4° in TA-GO correspond to the typical crystalline structure of AL and TA, respectively. Compared the XRD pattern of P-AL-GO/P-TA-GO, there was little change in the morphology after modification, suggesting that the phosphate-functionalization process did not alter the surface topography of the sample.

The SEM–EDS analysis imagines of U(VI)-loaded Al-GO/TA-GO, P-AL-GO/P-TA-GO are shown in Fig. 4. As indicated in the imagines, the U (VI) ions had been adsorbed onto the Al-GO/TA-GO, P-AL-GO/P-TA-GO successfully. Possible mechanisms of adsorption in our study could be the chelation of the adjacent phenolic hydroxyl groups to U (VI) ions. The principle components of the gels (O and C) are also presented in the SEM and EDS spectra. Moreover, the distribution of uranium in gels can be clearly observed on the mapping images.

The electro kinetic behavior of these gels in the solution represents one of the important properties of the adsorbent, and therefore is investigated in this study. The zeta potential analysis diagrams of AL-GO/TA-GO, P-AL-GO/P-TA-GO are shown in Fig. 5. Compared with the zeta potential diagrams of AL-GO/TA-GO, P-AL-GO/P-TA-GO have the higher negative zeta potentials, and their charge values range from -19.17 mV to -48.45 mV (for P-AL-GO), and − 6.71 mV to − 45.61 mV (for P-TA-GO), respectively. It also showed that the values of zeta potential charges greatly reduced and the amount of surface oxygen sites increased in the pH range used in our study. Such changes all indicate the successful implementation of the surface phosphorylation.

The surface charge of P-AL-GO/P-TA-GO is different at different pH values, which affects its affinity for U(VI). Influence of acidity (range from 3.5 to 6.5) on adsorption capacity (100 mg L^{-1}, 298 K) are presented in Fig. 6. The adsorption amount of U(VI) on P-AL-GO/P-TA-GO increased sharply with the increasing pH values. At lower pH values, the competition between H^+ and the positive uranium species such as UO_2^{2+}, $UO_2(OH)^+$, and $(UO_2)_3(OH)^{5+}$ increased and the active sites of adsorbents (–COOH and –OH groups) are protonated. When the pH value increased, the negative charged groups lead to the electrostatic repulsion between P-AL-GO/P-TA-GO and the positive uranium species. The number of H^+ also decreased at higher pH values, the competition between H^+ and positive uranium became less significant. The further increase of pH value will cause the precipitation of U(VI), a pH value of 5.5 was used in subsequent experiments.

The effect of contact time on the adsorption amount was assessed with an initial U (VI) concentration of 100 mg/L, pH of 6.0 at three different temperature, the results were plotted in Fig. 7. The uptake amount of uranium (VI) increased with longer contact time and attains adsorption equilibrium at about 120 min. Hence, the optimum contact time appears to be 120 min and used in the consequent experiments.

The experimental data of the adsorption of U (VI) on P-AL-GO/P-TA-GO gel were analyzed by applying the pseudo-first-order rate equation as in Eq. (2), the pseudo-second-order rate equation, Eq. (3), and internal diffusion rate equation, Eq. (4). The paths and mechanism of U (VI) ion adsorption on P-AL-GO/P-TA-GO gel were examined and discussed. These rate equations are expressed as follows:

$$\ln\left(q_e - q_t\right) = \ln q_e - K_1 t \tag{2}$$

$$\frac{t}{q_t} = \frac{1}{q_e}t + \frac{1}{k_2 q_e^2} \tag{3}$$

$$q_t = k_{id} t^{\frac{1}{2}} + C \tag{4}$$

The generated pseudo-second-order model (*t*/*qt* versus *t*) was given in the inset of Fig. 6. The kinetic parameters of three models are summarized in Table 1.

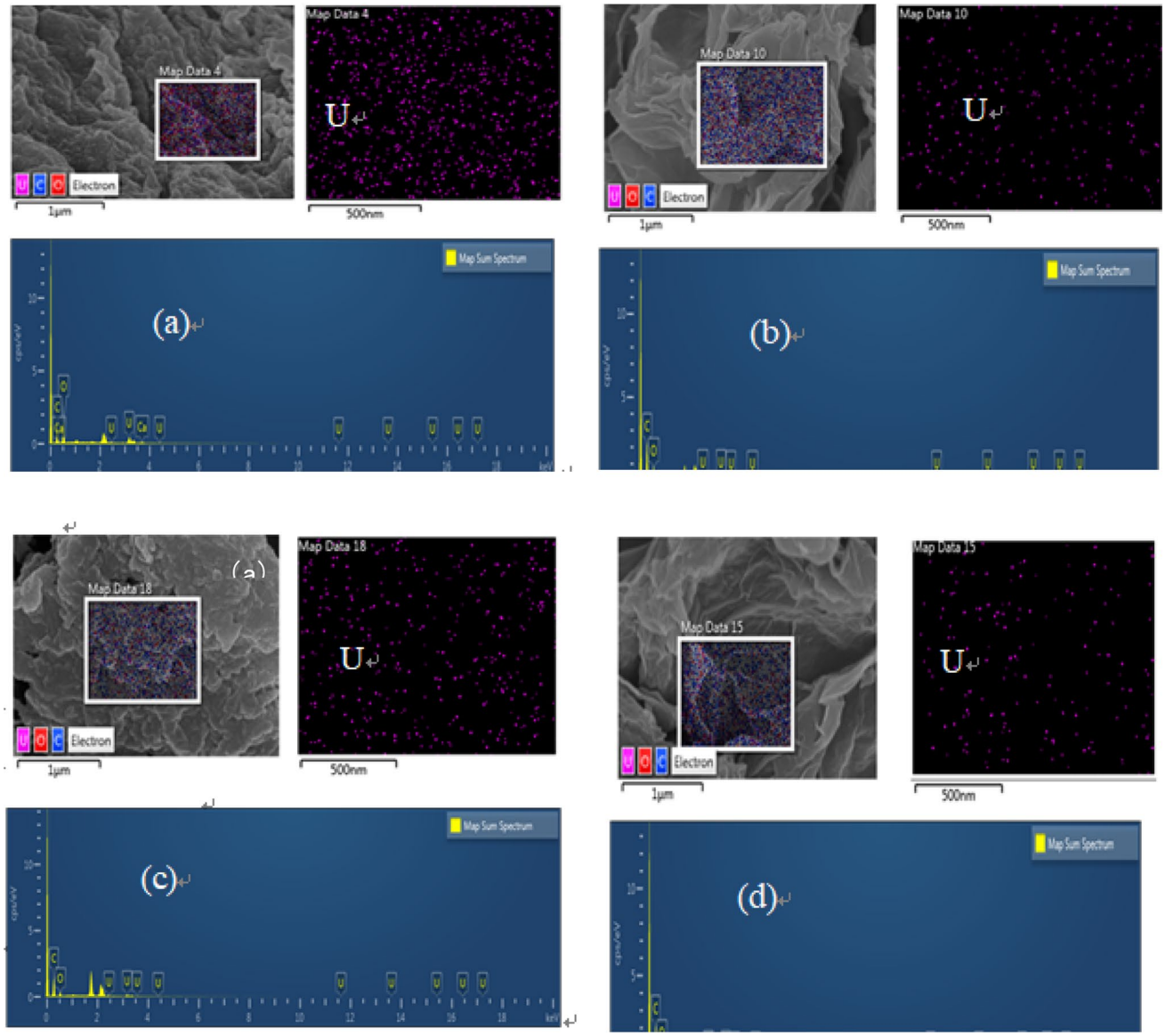

Fig. 4 SEM–EDS mapping of U(VI)-loaded Al-GO (**a**) /TA-GO (**b**), and P-AL-GO (**c**) /P-TA-GO (**d**)

As shown in Fig. 7, The correlation coefficient (R^2) suggests that pseudo-second-order kinetic model is best suitable for the adsorption process. The corresponding parameters in Table 1 show that the mechanism of adsorption process could be defined as chemisorption and was rate limiting step. It is necessary and critical to predict the equilibrium isotherm of U (VI) ion on the surface of adsorbent. The isothermal data were fitted by the commonly used Langmuir, Freundlich and Temkin isotherm models as written in the following equations (Eqs. (5–7)):

$$\frac{C_e}{q_e} = \frac{C_e}{q_m} + \frac{1}{q_m K_L} \tag{5}$$

$$\ln q_e = \ln K_F + \frac{1}{n} \ln C_e \tag{6}$$

$$q_e = \frac{RT}{b} \ln A + \frac{RT}{b} \ln C_e \tag{7}$$

The C_e versus q_e of U(VI) on P-AL-GO/P-TA-GO is showed in Fig. 8. The adsorption amount increased with increasing concentration, and the adsorption capacity reached saturation level. The Langmuir isotherm (C_e versus C_e/q_e) on P-AL-GO/P-TA-GO for the adsorption process are showed in the inset in Fig. 8. The Langmuir isotherm considers that the adsorption occurs on a monolayer

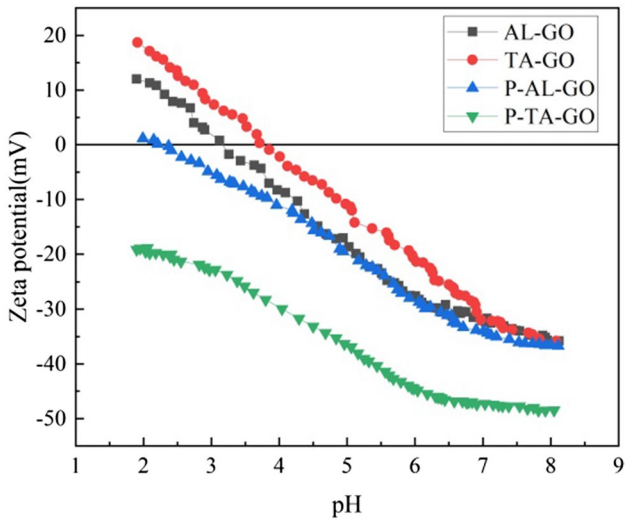

Fig. 5 Zeta potential of AL-GO/TA-GO, P-AL-GO/P-TA-GO as a function of pH

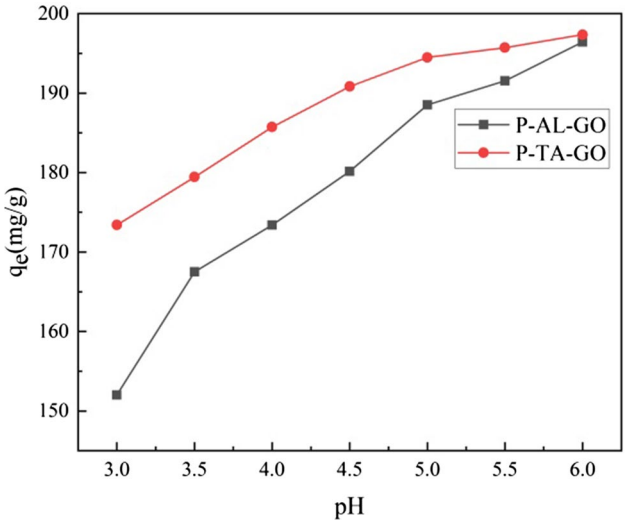

Fig. 6 Effect of solution pH

coverage with identical active sites in terms of energy on both adsorbents.

Table 2 shows the isotherm parameters calculated by the three isotherm models. As indicated by the values of R^2 the measured adsorption isotherms fit very well with the Langmuir model, suggesting the monolayer adsorption mechanism of U(VI) onto P-AL-GO/P-TA-GO surface. The maximum adsorption capacity for U(VI) on P-TA-GO estimated from Langmuir isotherm is higher than that of P-AL-GO (568.18 mg/g vs. 546.45 mg/g, respectively).

Table 3 provides the comparison of the adsorption capacities of the adsorbents prepared in this study with those reported in the recent literatures. As shown in the table, the adsorbents of P-AL-GO/P-TA-GO prepared in this study demonstrated much higher adsorption capacities of U(VI) from aqueous solution as compared with the reported adsorbents. So, they are two highly effective adsorbents.

The thermodynamic parameters of adsorption, including standard enthalpy (ΔH^0), standard entropy (ΔS^0) and Gibbs free energy (ΔG^0), are used to verify whether the adsorption process is spontaneous. The relationship among these parameters can be described by Eqs. (8) and (9):

$$\ln K_L = -\frac{\Delta H^0}{RT} + \frac{\Delta S^0}{R} \tag{8}$$

$$\Delta G^0 = \Delta H^0 - T\Delta S^0 \tag{9}$$

The slope and intercept of the inset in Fig. 9 give the values of $\Delta H°$ and $\Delta S°$, then the value of $\Delta G°$ was calculated from Eq. (8). The thermodynamic parameters obtained from the adsorption isotherm of pH 5.5 are presented in Table 4. The value of $\Delta G°$ decreases with the increase of temperature, which indicates that the adsorption of U (VI) is more favorable at higher temperature. The positive values of ΔH^0 suggest the endothermic nature, while the positive entropy change, ΔS^0, indicates the increase in the disorderness and randomness of the adsorption at the solid-solution interface. These characteristics of thermodynamic parameters reveal that P-AL-GO/P-TA-GO has good U (VI) adsorption performance.

Table 1 Corresponding data for the pseudo-first-order and pseudo-second-order models

Adsorbents	T	$q_{e,exp}$	Pseudo-first-order			Pseudo-second-order			Internal diffusion	
			k_1	$q_{e,cal}$	R^2	k_2	$q_{e,cal}$	R^2	k_{id}	R^2
	K	mg/g	1/min	mg/g		g/mg/min	mg/g		g/mg/min	
P-AL-GO	288	183.03	0.020	4.286	0.9638	1.32×10^{-4}	196.46	0.9971	0.558	0.6852
	298	188.74	0.019	5.053	0.9513	9.66×10^{-5}	199.60	0.9951	0.456	0.6178
	308	194.93	0.017	5.708	0.9061	7.65×10^{-5}	204.50	0.9971	0.599	0.6512
P-TA-GO	288	189.69	0.027	15.60	0.9157	2.12×10^{-4}	203.66	0.9915	2.010	0.8157
	298	194.20	0.028	35.17	0.9356	3.55×10^{-4}	206.19	0.9984	2.001	0.7478
	308	200.86	0.025	33.59	0.9081	8.79×10^{-4}	209.64	0.9944	2.093	0.7378

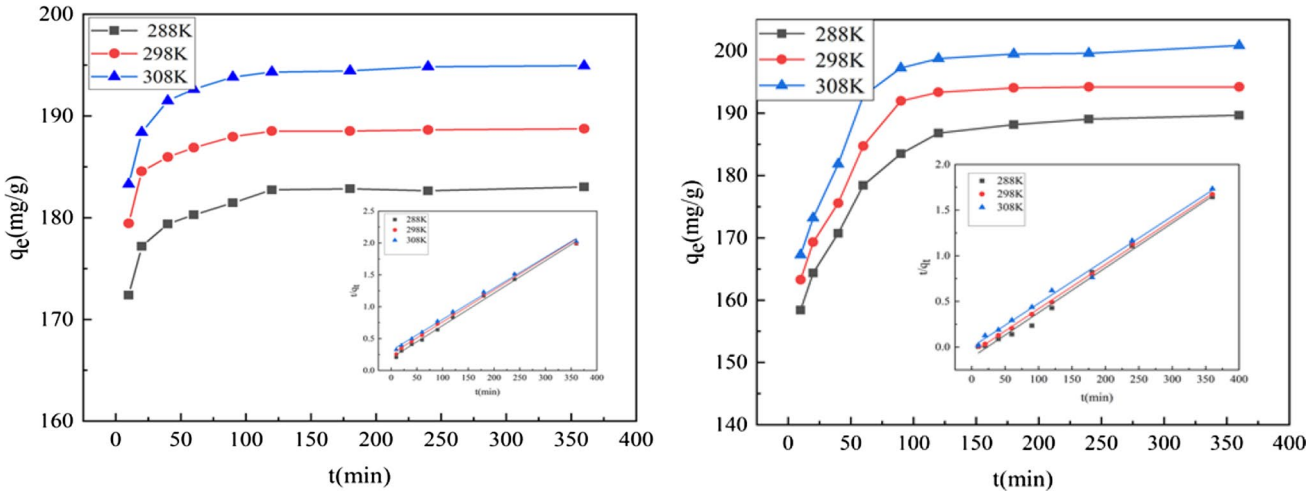

Fig. 7 Effects of contact time on adsorption amount for P-AL-GO (left)/P-TA-GO (right); Inset shows the linearized pseudo-second-order plot

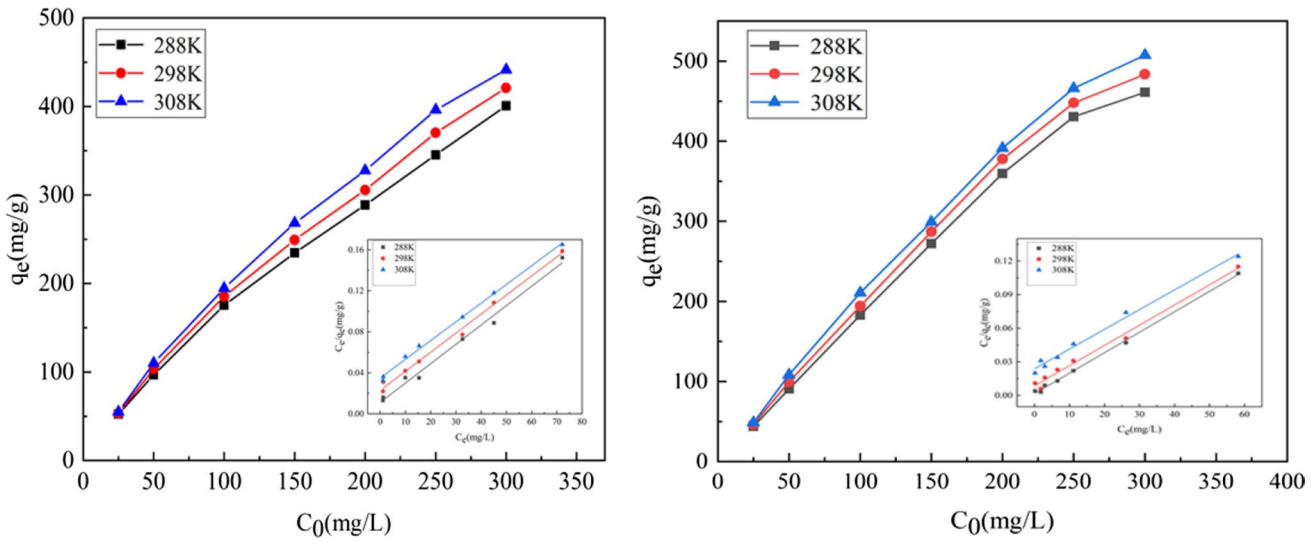

Fig. 8 Influences of initial concentration on adsorption amount for P-AL-GO (left)/P-TA-GO (right); Inset shows the linearized Langmuir plot

Table 2 Parameters of Langmuir, Freundlich and Temkin isotherms

Adsorbents	T	$q_{m,exp}$	Langmuir			Freundlich			Temkin		
			$q_{m,cal}$	K_d	R^2	K_F mg/g	n	R^2	A	b	R^2
	K	mg/g	mg/g	L/mg					L/g	J/mol	
P-AL-GO	288	400.64	529.10	0.169	0.9904	50.343	2.079	0.9091	1.998	32.109	0.9649
	298	420.98	537.63	0.081	0.9939	64.974	2.263	0.933	1.970	31.266	0.9659
	308	441.62	546.45	0.052	0.9971	89.914	2.073	0.9475	1.958	30.365	0.9698
P-TA-GO	288	460.97	549.45	0.273	0.9978	112.323	3.012	0.9131	4.847	31.281	0.8014
	298	483.54	555.56	0.210	0.9908	147.363	3.098	0.9227	4.993	31.257	0.7961
	308	507.38	568.18	0.074	0.9910	194.605	3.235	0.9319	5.139	31.260	0.7935

Table 3 Summary of the U(VI) adsorption capacities of various adsorbents

Material	pH	Temp.(K)	Equilibrium time (min)	Adsorption capacity (mg g^{-1})	References
GO @ chitosan	5.0	313	150	204.1	[18]
GO @ cellulose	5.0	303	150	101.0	[19]
UiO-66 @ amidoxime	5.5	313	800	227.8	[20]
mesoporous silica @ amidoxime	5.0	298	120	277.3	[21]
GO-CS-AO/GO-CMC-AO	6.0	308	120	248.75/327.86	[16]
P-AL-GO/P-TA-GO	5.5	298	120	546.45/568.18	This study

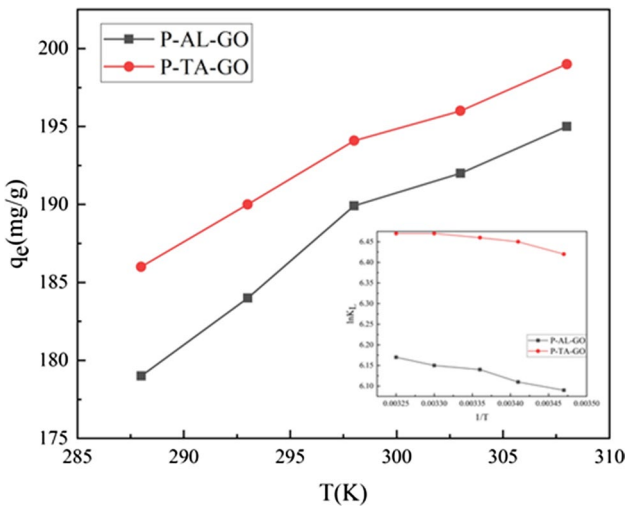

Fig. 9 Van't Hoff plots for the uptake of U(VI)

Distribution coefficients (K_d) and distribution selectivity coefficient ($S_{U/M}$) were employed to evaluate the adsorption selectivity of P-AL-GO/P-TA-GO, and they were calculated using Eqs. (10, 11):

$$K_d = \frac{C_0 - C_e}{C_e} \times \frac{V}{m} \tag{10}$$

$$S_{U/M} = \frac{k_{d,U}}{k_{d,M}} \tag{11}$$

The impacts of coexistence of Nd(III), La(III), Ce(III), Sr(II), Ni(II)), Co(II), and Ba(II) on P-AL-GO/P-TA-GO adsorption process of U(VI) are investigated. The results are plotted in Fig. 10. All the experiments were performed under the conditions of pH 5.5, m/V = 0.5 g/L, C_0 = 100 mg/L at 298 K. As shown in the Fig. 10, P-AL-GO/P-TA-GO have higher K_d and $S_{U/M}$ values than that of AL-GO/TA-GO. Such high adsorption selectivity is mainly due to the phosphoric acid groups grafted, which indicates that the phosphate-functionalization promotes the selective adsorption of U(VI) over coexisting ions.

Based on kinetics results in the current study, it could be observed that the adsorption process might be considered as chemisorption and was rate-limiting step [22]. Data obtained from isotherms indicated that the adsorption process was temperature independent and occurred onto monolayer surface (Langmuir isotherm) [23]. EDS analysis imagines after adsorption showed that possible mechanisms of adsorption could be the chelation of the adjacent phenolic hydroxyl groups to U(VI) ions. Thermodynamic parameters obtained demonstrated that the adsorption process was endothermic and spontaneous [24]. The phosphate-functionalized biopolymer/graphene oxide gels could be regarded as excellent adsorbents with high selectivity for uranium adsorption over coexisting ions because phosphoryl groups had the high affinity to uranium.

The regeneration of the loaded adsorbents was performed to explore the possibility to reduce the operating cost and minimizing waste disposal. Figure 11 shows the adsorption efficiency over the numbers of recycle time, where the spent P-AL-GO/P-TA-GO were regenerated with 0.1 M HNO_3 solution as the desorption agent. As shown in Fig. 11, the adsorption capacities decreased slowly with increasing recycle times. The adsorption capacity remained steady at over 90% of the fresh adsorbent in the first four regeneration cycles, and then decreased at

Table 4 Thermodynamic constants for adsorption of U(VI)

Adsorbents	ΔH^0kJ/mol	ΔS^0J/(mol.k)	ΔG^0(kJ/mol)				
			288 K	293 K	298 K	303 K	308 K
P-AL-GO	2.96	60.91	14.58	− 14.89	− 15.19	− 15.49	− 15.80
P-TA-GO	1.79	59.66	− 15.39	− 15.69	− 15.99	− 16.29	− 16.58

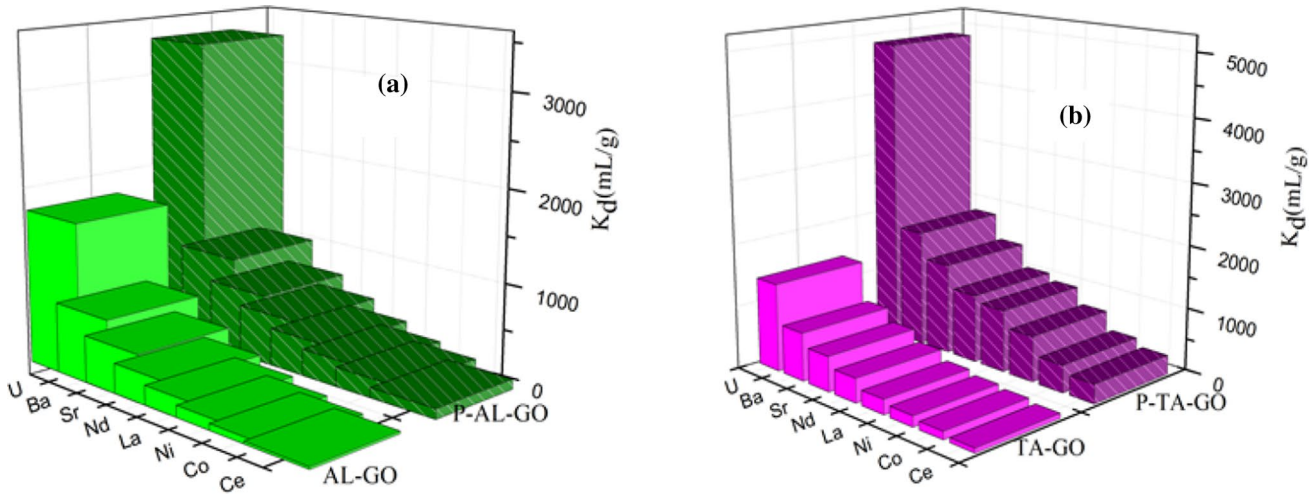

Fig. 10 Selective adsorption on Al-GO/P-Al-GO (**a**), Ta-GO/P-Ta-GO (**b**) towards multiple metal ions

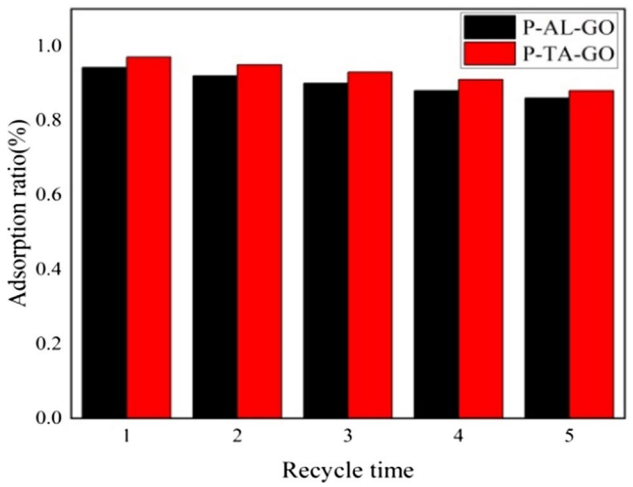

Fig. 11 Influence of recycle time of P-AL-GO/ P-TA-GO

the fifth cycle. The good performance of the regenerated P-AL-GO/P-TA-GO demonstrates great promise for their potential applications in the field of U (VI) adsorption.

Conclusions

The properties of phosphoric acid functionalized biopolymer/graphene oxide gels and their applications in adsorption and separation of uranium (VI) in aqueous solution were investigated in this study. The results of FTIR, XRD, SEM, and EDS measurement and analysis indicated the successful synthesis of P-AL-GO/P-TA-GO adsorbents. The effects of contact time and solution pH values on the adsorption of U(VI) onto P-AL-GO/P-TA-GO were studied, and the optimum conditions were pH of solution 5.5 and contact time 120 min. The maximum adsorption capacity for U(VI) on P-TA-GO estimated from Langmuir isotherm is higher than that of P-AL-GO (568.18 mg/g vs. 546.45 mg/g, respectively). The batch adsorption study revealed that the adsorption process followed pseudo-second-order kinetics ($R^2 > 0.99$ for both P-AL-GO and P-TA-GO), pointing to a chemisorption dominating mechanism. The thermodynamic parameters calculated from the temperature dependent isotherms suggested that the adsorption process was endothermic and spontaneous. The experiments were also carried out for the adsorption selectivity study, the results showed that the P-AL-GO/P-TA-GO had very good selectivity to U(VI) ions over the coexisting ions.

Acknowledgements The present work was partially supported by the national science foundation of China (21866005), Jiangxi Key plan of research and development (20192BBH80011).

Declarations

Conflict of interest The authors declare that they have no conflicts interest.

References

1. He Y, Lin XY, Yan TS, Zhang XN, Luo XG (2018) Selective adsorption of uranium from salt lake-simulated solution by phenolic-functionalized hollow sponge-like adsorbent. J Chem Technol Biot 49(2):455–467
2. Banerjee C, Dudwadkar N, Tripathi SC, Gandhi PM, Grover V, Kaushik CP, Tyagi AK (2014) Nano-cerium vanadate: a novel inorganic ion exchanger for removal of americium and uranium from simulated aqueous nuclear waste. J Hazard Mater 280:63–70

3. Chen QY, Yao Y, Li XY, Lu J, Zhou J, Huang ZL (2018) Comparison of heavy metal removals from aqueous solutions by chemical precipitation and characteristics of precipitates. J Water Process Eng 26:289–300
4. Vázquez-Campos X, Kinsela AS, Collins RN, Neilan BA, Waite TD (2017) Uranium extraction from a low-grade, stockpiled, non-sulfidic ore: Impact of added iron and the native microbial consortia. Hydrometallurgy 167:81–91
5. Luo W, Xiao G, Tian F, Richardson JJ, Wang YP, Zhou JF, Guo JL, Liao XP, Shi B (2019) Engineering robust metal–phenolic network membranes for uranium extraction from seawater. Energy Environ Sci 12(2):607–614
6. Bhat SV, Melo JS, Chaugule BB, D'Souza SF (2008) Biosorption characteristics of uranium(VI) from aqueous medium onto Catenella repens, a red alga. J Hazard Mater 158(2):628–635
7. Rana D, Matsuura T, Kassim MA, Ismail AF (2013) Radioactive decontamination of water by membrane processes: a review. Desalination 321:77–92
8. Chen X, Zhou SK, Zhang LM, You TT, Xu F (2016) Adsorption of heavy metals by graphene oxide/cellulose hydrogel prepared from NaOH/Urea aqueous solution. Materials 9(7):582
9. Liu HJ, Zhou YC, Yang YB, Zou K, Wu RJ, Xia K, Xie SB (2019) Synthesis of polyethylenimine/graphene oxide for the adsorption of U(VI) from aqueous solution. Appl Surf Sci 471:88–95
10. Huang GL, Peng W, Yang SS (2018) Synthesis of magnetic chitosan/graphene oxide nanocomposites and its application for U(VI) adsorption from aqueous solution. J Radioanal Nucl Chem 317:337–344
11. Rouf TB, Kokini JL (2016) Biodegradable biopolymer–graphene nanocomposites. J Mater Sci 51(22):9915–9945
12. Wang Y, Li ZH, Wang J, Li JH, Lin YH (2011) Graphene and graphene oxide: biofunctionalization and applications in biotechnology. Trends Biotechnol 29(5):205–212
13. Huang GL, Peng W, Yang SS (2018) Synthesis of magnetic chitosan/graphene oxide nanocomposites and its application for U(VI) adsorption from aqueous solution. J Radioanal Nucl Chem 317(1):337–344
14. Peng W, Huang GL, Yang SS, Guo CL, Shi J (2019) Performance of biopolymer/graphene oxide gels for the effective adsorption of U(VI) from aqueous solution. J Radioanal Nucl Chem 322:861–868
15. Anirudhan TS, Suchithra PS (2008) Synthesis and characterization of tannin-immobilized hydrotalcite as a potential adsorbent of heavy metal ions in effluent treatments. Appl Clay Sci 42(1):214–223
16. Yang SS, Huang YW, Huang GL, Peng W, Guo CL (2020) Jeffery Shi preparation of amidoxime-functionalized biopolymer/graphene oxide gels and their application in selective adsorption separation of U(VI) from aqueous solution. J Radioanal Nucl Chem 324:847–855
17. Liu Y, Zhao ZP, Yuan DZ, Wang Y, Dai Y, Zhu Y, Chew JW (2019) Introduction of amino groups into polyphosphazene framework supported on CNT and coated Fe3O4 nanoparticles for enhanced selective U(VI) adsorption. Appl Surf Sci 466:893–902
18. Zhuang ST, Cheng R, Kang M, Wang JL (2018) Kinetic and equilibrium of U(VI) adsorption onto magnetic amidoxime-functionalized chitosan beads. J Clean Prod 188:655–661
19. Yang A, Wu J, Huang CP (2018) Graphene oxide-cellulose composite for the adsorption of Uranium(VI) from dilute aqueous solutions. J Hazard Toxic Radioact Waste 22:65–73
20. Liu JM, Yin XH, Liu T (2018) Amidoxime-functionalized metal-organic frameworks UiO-66 for U(VI) adsorption from aqueous solution. J Taiwan Inst Chem E 95:416–423
21. Wang FH, Li HP, Liu Q, Li ZS, Li RM, Zhang HS, Liu LH, Emelchenko GA, Wang J (2016) A graphene oxide/amidoxime hydrogel for enhanced uranium capture. Sci Rep-UK 6:19367
22. Nuhanović M, Smječanin N, Mulahusić N, Sulejmanović J (2021) Pomegranate peel waste biomass modified with H_3PO_4 as a promising sorbent for uranium(VI) removal. J Radioanal Nucl Ch. https://doi.org/10.1007/s10967-021-07664-5
23. Nuhanović M, Smječanin N, Curić N, Vinković A (2021) Efficient removal of U(VI) from aqueous solution using the biocomposite based on sugar beet pulp and pomelo peel. J Radioanal Nucl Ch. https://doi.org/10.1007/s10967-021-07651-w
24. Noli F, Kapashi E, Kapnisti M (2019) Biosorption of uranium and cadmium using sorbents based on Aloe vera wastes. J Environ Chem Eng 7(2):102985